Acta Cryst. (1969). A25, 43

Profile Analysis in Single Crystal Diffractometry

BY R. DIAMOND

Medical Research Council, Laboratory of Molecular Biology, Hills Road, Cambridge, England

It is shown that a suitable curve fitting procedure can reduce the standard deviation of intensity measurements made with a scanning diffractometer except when the intensity is large in relation to the background level. The procedure has been implemented with an Arndt–Phillips linear diffractometer, on-line to a Ferranti Argus 312 computer. The shape of the profile which is fitted to the observed profile is learnt and continually revised. In typical cases the standard deviation of the intensity, as determined from counting statistics alone, is about 0·4–0·6 times that given by alternative methods. In addition to profile fitting, a straightforward peak-minus-background treatment is always done, and the two results are compared. This enables a large measure of internal consistency checking to be done, so that certain types of error condition can be detected. Criteria are also developed whereby the better of the two results may be chosen in each case, having regard to such parameters as the peak to background ratio and the closeness of fit accomplished in profile fitting.

1. Introduction

The Arndt–Phillips linear diffractometer as normally marketed is equipped to measure X-ray reflexions by scanning on ω (*i.e.* rotating the crystal with the slides stationary) with a stationary-crystal measurement of the background level at each end at the scan. This method of measurement involves only three measurements and will be referred to here as the background-peak-background (BPB) method. This procedure is only optimal if the peak exactly fills the angular width of the scan (the frame width), and this condition cannot be realized in practice because the peak varies a little in both width and position within the frame from place to place in reciprocal space. It may be necessary, for example, to use a 2° scan for a crystal giving peaks 1° wide to be certain that the whole of the peak falls within the 2° scan for every reflexion. For purposes of comparison with other methods it is convenient to suppose that the crystal continues to move during the background measurements, so that this circumstance is exactly equivalent to a 4° scan in which the peak is required to fall within the central 2°. In such a case the BPB method is very far from optimal.

We shall describe in this paper a pair of methods which complement one another in their characteristics and which jointly are always optimal, such that in the conditions of the above example the whole of the available counting time would be spent in the central 2° with very appreciable gain in accuracy. The only requirements are that the whole of the peak shall be within the scanned range which is now 2° (though the position of its centre is immaterial), and ideally the frame width should be about twice the peak width, or a little less, though the consideration of positional uncertainty of the peak is usually the over-riding one. In order to achieve this it is necessary to subdivide the scan into a number of small steps and to measure the counts associated with each step. Effectively, this means that the diffractometer must be on-line to a computer. The techniques employed to transmit the individual measurements direct to the core store of a computer are due to Arndt and Phizackerley and will be described elsewhere.

The technique has been developed on a linear diffractometer fitted with three counters to measure three levels of reciprocal space simultaneously. Because of the curvature of the Ewald sphere, the three reflexions do not reach their maxima quite simultaneously, and therefore the frame width needs to be a little larger than would be required for a single counter instrument. This fact sets the BPB method at a further disadvantage in relation to the new technique.

The pair of methods for on-line application will be referred to below as *A* and *B*. *A* is particularly valuable when the peak/background ratio is low and *B* is preferable when it is high. Together they are ideally suited to neutron diffraction or to X-ray diffraction from proteins where reflexions with a low peak to background ratio are common. However, the method depends for its success on there being a number of fairly strong reflexions among the weaker ones, from which the shape of the learnt profile may be updated, and it assumes that the ideal profile of a weak reflexion differs from that of a strong reflexion only by a scale factor.

The program processes data from all three counters in under a second and uses about 2K of core store (24 bit words).

2. Theoretical survey

2·1. *Random errors*

In any diffractometer in which measurements are made by oscillating the crystal through a small angle the integrated intensity may always be written as

$$I = I(y_1, y_2, \ldots y_N), \qquad (1)$$

in which the y_i represent the counts collected at each of a series of small steps or intervals of the oscillation angle, and the function I is designed to subtract out the background level.

It follows therefore that

$$\delta I = \sum_i \frac{\partial I}{\partial y_i}\delta y_i$$

$$(\delta I)^2 = \sum_i \sum_j \frac{\partial I}{\partial y_i}\frac{\partial I}{\partial y_j}\delta y_i \delta y_j$$

and, using $\langle\ \rangle$ to denote expected value, we have for the variance on I

$$\sigma^2(I) = \langle(\delta I)^2\rangle = \sum_i \sum_j \frac{\partial I}{\partial y_i}\frac{\partial I}{\partial y_j}\langle\delta y_i \delta y_j\rangle ,$$

and since the individual ordinates y_i are statistically independent and the $\sqrt{n}$ law for Poisson distributions applies,

$$\left.\begin{aligned}\langle\delta y_i \delta y_j\rangle &= y_i \quad i=j\\ &= 0 \quad i\neq j\end{aligned}\right\} \tag{2}$$

and

$$\sigma^2(I) = \sum_i \left(\frac{\partial I}{\partial y_i}\right)^2 y_i \tag{3}$$

It is our purpose in what follows to show how the function I may be chosen to reduce $\sigma(I)$ in relation to conventional methods, and at the same time meet the requirement that I shall represent the integrated intensity with the background removed.

We suppose that the observations can be represented by

$$\mathbf{y}_{obs} = \mathbf{h}_1\mu_1 + \mathbf{h}_2\mu_2 , \tag{4}$$

in which $\mathbf{h}_1$ is a column vector whose elements are all $1/N$, $\mathbf{h}_2$ is a column vector representing the shape of the observed profile, normalized so that

$$\sum_{i=1}^{N} h_{1i} = \sum_{i=1}^{N} h_{2i} = 1 ; \tag{5}$$

then μ_1 is the integrated background and μ_2 is the integrated peak. Then if we fit to this a calculated profile

$$\mathbf{y}_{calc} = \mathbf{g}_1\lambda_1 + \mathbf{g}_2\lambda_2 \tag{6}$$

by the method of least squares, with $\mathbf{g}_1 = \mathbf{h}_1$ and $\mathbf{g}_2$ representing a peak normalized to unity, then provided $\mathbf{g}_2$ is compatible with $\mathbf{h}_2$ the value of λ_2 so found is a measure of the integrated intensity. We begin by considering the dependence of $\sigma(I)$ on $\mathbf{g}_1$, $\mathbf{g}_2$, $\mathbf{h}_1$, $\mathbf{h}_2$, μ_1 and μ_2 and the compatibility of $\mathbf{g}_2$ with $\mathbf{h}_2$. In the first place we ascribe unit weight to each y_i and later introduce weights to represent the smaller proportional error (larger absolute error) of the larger ordinates.

Within the restriction of equal observational weights it is possible to write down expressions for I and $\sigma^2(I)$. These are derived in Appendix B and summarized in Table 1.

Case A is general and may be applied to other examples not given in the table.

Case B is, in fact, the peak-minus-background type of measurement in which m ordinates are supposed to be in the peak and n are taken to be pure background. This method has the outstanding property that provided h_2 vanishes in the background region where g_2 vanishes, $\tilde{\mathbf{g}}_2\mathbf{h}_2 = \tilde{\mathbf{g}}_2\mathbf{g}_2$ so that it yields $I=\mu_2$ in all circumstances. It is therefore the safest with regard to systematic error. Any other form for g_2 yields $I=\mu_2$ only if $\tilde{\mathbf{g}}_2\mathbf{h}_2 = \tilde{\mathbf{g}}_2\mathbf{g}_2$, which occurs if $\mathbf{g}_2 = \mathbf{h}_2$ and in certain other special cases considered in Appendix A.

The general case A may be compared with case B using Schwarz's inequality in the form

$$(\tilde{\mathbf{f}}_1\mathbf{f}_2)^2 \leq \tilde{\mathbf{f}}_1\mathbf{f}_1\tilde{\mathbf{f}}_2\mathbf{f}_2 , \tag{7}$$

$\mathbf{f}_1$ and $\mathbf{f}_2$ being column vectors of dimension N, then provided $\mathbf{g}_2$ has m elements non-zero and $n=N-m$ which are zero; then setting

Table 1. *Summary of expressions for I and $\sigma^2(I)$*

$\mathbf{g}_2$ and $\mathbf{h}_2$ are column vectors and the tilde denotes transposition. $\tilde{\mathbf{g}}_2^2$ is a row vector whose ith element is the square of the ith element of $\tilde{\mathbf{g}}_2$. In case C the working range of the continuous variable x is $|x|\leq a$, and the functions are supposed to be sampled at regular intervals of $2a/N$

Case	$\mathbf{g}_2$	$\mathbf{h}_2$	I	$\sigma^2(I)$
A	Any	Any	$\mu_2\dfrac{N\tilde{\mathbf{g}}_2\mathbf{h}_2 - 1}{N\tilde{\mathbf{g}}_2\mathbf{g}_2 - 1}$	$\mu_1\dfrac{1}{N\tilde{\mathbf{g}}_2\mathbf{g}_2-1} + \mu_2\dfrac{1-2N\tilde{\mathbf{g}}_2\mathbf{h}_2+N^2\tilde{\mathbf{g}}_2^2\mathbf{h}_2}{[N\tilde{\mathbf{g}}_2\mathbf{g}_2-1]^2}$
B	$g_2=1/m$ for m ordinates. $g_2=0$ for remaining $n=N-m$ ordinates	Any provided $h_2=0$ when $g_2=0$	μ_2	$\mu_1\dfrac{m}{n}+\mu_2$
C	$\dfrac{2a}{Np}\exp(-\pi x^2/p^2)$	$\dfrac{2a}{Nq}\exp(-\pi x^2/q^2)$	$\mu_2\dfrac{2a\sqrt{\frac{2p^2}{p^2+q^2}}-p\sqrt{2}}{2a-p\sqrt{2}}$	$\mu_1\dfrac{1}{2a/p\sqrt{2}-1} + \mu_2\dfrac{1-\frac{4a}{\sqrt{p^2+q^2}}+\frac{4a^2}{p\sqrt{p^2+2q^2}}}{[2a/p\sqrt{2}-1]^2}$

$$\mathbf{f}_1=\mathbf{g}_2 \quad \text{and} \quad f_2=1/m \quad \text{where} \quad g_2\neq 0$$
$$f_2=0 \quad \text{where} \quad g_2=0$$

gives

$$\tilde{\mathbf{g}}_2\mathbf{g}_2 \geq 1/m \,. \tag{8}$$

Setting $\mathbf{f}_1=\mathbf{g}_2^{1/2}$, $\mathbf{f}_2=\mathbf{g}_2^{3/2}$ gives

$$(\tilde{\mathbf{g}}_2\mathbf{g}_2)^2 \leq \tilde{\mathbf{g}}_2^2\mathbf{g}_2 \tag{9}$$

(in which we mean the ith power of a vector to be read as a vector each element of which is the ith power of the corresponding element). Accordingly, in the general case A, if $\mathbf{g}_2$ has been chosen equal to $\mathbf{h}_2$ (which is the only important case), we see from the Table that

$$\left.\begin{aligned} &\sigma^2(I)=\mu_1\frac{m}{\alpha n}+\mu_2\beta\,, \\ &\text{in which} \\ &\alpha=\frac{m}{n}(N\tilde{\mathbf{g}}_2\mathbf{g}_2-1)\geq 1 \\ &\text{and} \\ &\beta=\frac{1-2N\tilde{\mathbf{g}}_2\mathbf{g}_2+N^2\tilde{\mathbf{g}}_2^2\mathbf{g}_2}{1-2N\tilde{\mathbf{g}}_2\mathbf{g}_2+N^2(\tilde{\mathbf{g}}_2\mathbf{g}_2)^2}\geq 1 \end{aligned}\right\} \tag{10}$$

α and β being unity in case B.

We conclude that if the peak to background ratio

$$\frac{\mu_2}{\mu_1} < \frac{m}{n}\,\frac{1-1/\alpha}{\beta-1} \tag{11}$$

then, with the foregoing conditions and assumptions, fitting the profile g_2 to the observations will lead to a smaller variance on the resulting integrated intensity than would method B, which is the classical peak-minus-background method. This may, in fact, occur with proteins for all except the strongest reflexions for which the converse argument applies. The advantage, of course, arises from the excess of α over unity.

These points are illustrated by case C in Table 1, in which both the observed and fitted profiles are assumed to be Gaussian of widths p and q in $|x|\leq a$. (It is never assumed that real profiles are Gaussian, and this example is only given to indicate the characteristics to be expected.) The numbers m and n do not occur in these expressions because there is intrinsically no point in the working range at which the peak region is distinguished from the background region. In order to make a quantitative comparison we note that

$$\int_{-\tau}^{\tau}\frac{1}{\sqrt{2\pi}}\exp(-t^2/2)dt=0{\cdot}990\,, \quad \tau=2{\cdot}57$$
$$=0{\cdot}999\,, \quad \tau=3{\cdot}27$$

so that if the peak region of the working range, $2am/(m+n)$, is set to contain all but 1% of the diffraction peak, or all but 0·1%, then effectively

$$\frac{a\sqrt{2}}{p}=\frac{(m+n)\tau}{m\sqrt{\pi}}$$

for the case $p=q$ and the appropriate values of τ. For the 0·1% case this gives

$$\sigma^2(I)=\frac{\mu_1 m/n}{1{\cdot}84+0{\cdot}84\ m/n}+\mu_2\left[1+\frac{0{\cdot}15(m+n)^2}{(0{\cdot}46\ m+n)^2}\right]$$

and if a is such that this setting of τ results in $m=n$ this corresponds to $\alpha=2{\cdot}68$, $\beta=1{\cdot}29$. At the 1% level and with the same assumptions (involving a different a) $\alpha=1{\cdot}90$, $\beta=1{\cdot}36$. Corresponding values of μ_2/μ_1 below which profile fitting is advantageous are, by equation (11), 2·16 and 1·31.

2.2. *Systematic errors.*

The expression

$$I=\lambda_2=\mu_2\frac{N\tilde{\mathbf{g}}_2\mathbf{h}_2-1}{N\tilde{\mathbf{g}}_2\mathbf{g}_2-1} \tag{12}$$

shows that if $\tilde{\mathbf{g}}_2\mathbf{h}_2\neq\tilde{\mathbf{g}}_2\mathbf{g}_2$ then systematic errors are incurred in taking λ_2 as our measure of μ_2. Fig. 1 shows contours of λ_2/μ_2 corresponding to case C as a function of the ratios a/p and q/p. These curves serve to show the importance of matching the width p of the fitted profile to the width q of the observed profile. If $q/p=1{\cdot}1$, for example, then the result, λ_2, will be $\sim 6\%$ low if $a/p=4{\cdot}0$ or $\sim 10\%$ low if $a/p=1{\cdot}4$. If this effect is not to offset the available advantage in random error, it is essential that good matching of widths be achieved. At first sight there appear to be two possible approaches to the problem of avoiding systematic error in curve fitting. One of these is to arrange, by a learning process or otherwise, that $\mathbf{g}_2=\mathbf{h}_2$, and the other approach is to fit to the observed curve a linear combination of several normalized curves $\mathbf{g}_i$ of different shapes, taking the sum of their coefficients as representing the integrated intensity, with the hope that such a linear combination may be able to represent $\mathbf{h}_2$ sufficiently closely even if this is not known in advance. This possibility is studied in detail in Appendix A where it is proved that the twin objectives of minimizing $\sigma^2(I)$ and avoiding systematic error by using several $\mathbf{g}_i$ are mutually exclusive, despite the fact that it *is* possible to use several $\mathbf{g}_i$ without enlarging $\sigma^2(I)$.

We conclude that the only practical way to proceed if the best advantage is sought, is to arrange for $\mathbf{g}_2$ to equal $\mathbf{h}_2$ and to fit this single curve.

2·3. *Weighted observations, comparison with the unweighted case*

Since the individual ordinates y_i have differing accuracies it follows from equation (2) that in fitting y_{calc} to y_{obs} the proper residual to minimize is

$$R=\Sigma\,(y_{\text{obs}}-y_{\text{calc}})^2/y_{\text{obs}}\,. \tag{13}$$

If we write

$$\mathbf{W}=\text{diag}\ \mathbf{y}_{\text{obs}}^{-1} \tag{14}$$

and let the ith element of $\mathbf{W}$ be $\omega_i=(1/y_i)_{\text{obs}}$ then if

$\boldsymbol{\varepsilon}=\mathbf{y}_{obs}-\mathbf{y}_{calc}$ the residual $R=\tilde{\boldsymbol{\varepsilon}}\mathbf{W}\boldsymbol{\varepsilon}$ is minimized by

$$\boldsymbol{\lambda}=(\tilde{\mathbf{G}}\mathbf{W}\mathbf{G})^{-1}\tilde{\mathbf{G}}\mathbf{W}\mathbf{y}_{obs}$$

where $\mathbf{G}=(\mathbf{g}_1,\mathbf{g}_2)$. But every element of the column $\mathbf{Wy}$ is unity, and since $\mathbf{g}_1$ and $\mathbf{g}_2$ are normalized

$$\begin{pmatrix}\lambda_1\\ \lambda_2\end{pmatrix}=(\tilde{\mathbf{G}}\mathbf{W}\mathbf{G})^{-1}\begin{pmatrix}1\\ 1\end{pmatrix}. \qquad (15)$$

Note that the situation is now basically different in that the observational quantities enter only as their reciprocals and only through the normal matrix. This complicates any satisfactory analysis of the characteristics of the system because the contributions of μ_1 and μ_2 to $\sigma^2(I)$ are no longer separable, and since the normal matrix is now data-dependent the properties of its inverse cannot be studied in terms of the fitted curves alone.

However, an expression for the variance derived from equation (3) may be given and is

$$\sigma^2(I)=D^{-2}\sum_i \omega_i^3\left[1-Ng_{2i}-I\frac{\partial D}{\partial \omega_i}\right]^2, \qquad (16)$$

in which $I=\lambda_2$ in equation (15), as before, and

$$D=\sum_i \omega_i \,.\, \sum_i \omega_i g_{2i}^2-\left(\sum_i \omega_i g_{2i}\right)^2$$

$$\frac{\partial D}{\partial \omega_i}=\sum_j \omega_j g_{2j}^2+g_{2i}^2\sum_j \omega_j-2g_{2i}\sum_j \omega_j g_{2j}$$

$$\sigma^2(\omega_i)=\omega_i^3 .$$

A number of comparative tests have been made between a weighted and an unweighted curve fitting procedure. In these tests the data and the g functions used were identical, and in most cases it was found that the

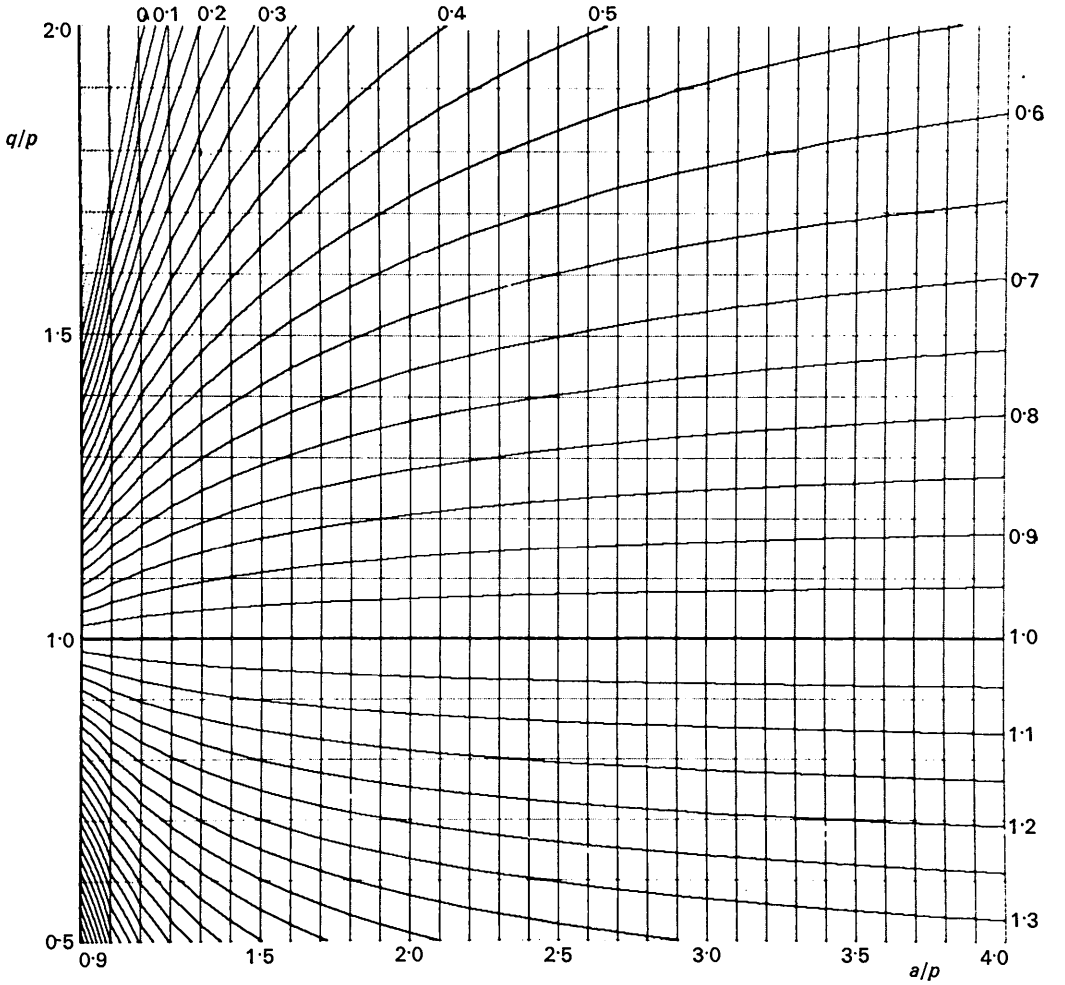

Fig. 1. Contours of the systematic error factor λ_2/μ_2 for a Gaussian of width p fitted to one of width q in $|x|\leq a$, as defined in Table 1, as a function of a/p and q/p, for an unweighted least-squares fitting. The contours are at intervals of 0·05, the unity contour being a straight line. The diagram was prepared by the method of Gossling (1967).

variance given by equation (16) for the weighted case was smaller than that given by equation (3) for the unweighted case; the only exceptions to this occurred with peaks which were both extremely strong and badly fitted, but such cases are dealt with by method *B* (see below) for which the question of weighting does not arise. Furthermore, the weighted case was less susceptible to systematic error due to mismatching of peak widths. For both these reasons, and because the residual (13) is the correct one, it was decided to implement the method in the weighted form, assuming that the characteristics of such a scheme are not worse than those of the un-weighted scheme which has been extensively studied.

3. Implementation

3·1. *Procedure*

The procedure which has been implemented uses equations (15) and (16) and learns a function g_2 from the observations as successive reflexions are processed. The sequence is as follows:

(i) The median of the observed peak is located using a pre-set number of ordinates either side of the centre.

(ii) The observations are folded about the median so that the ith and $(i+1)$th ordinates are added, as are the $(i-1)$th and $(i+2)$th *etc.* The median is not generally at the centre of the working range, so that some ordinates near one extreme have no corresponding ordinate the other side of the median, these ordinates are in the background region however, and are added together in pairs, so that at this stage we have $N/2$ ordinates representing the peak from edge to centre.

The purpose of this step is to eliminate the anti-symmetric component of the profile, which contributes nothing to the integrated intensity but would contribute to the residual (13) if not removed or allowed for, and this residual is used at a later stage. This folding is valid provided that the median is not too near the end of the working range (a condition which can be detected and flagged) and it allows for the background to be sloping or for the peak to be off-centre but becomes invalid if both these conditions arise at once (because the background integral λ_1 corresponds to the background level at the middle of the working range rather than at the median of the peak).

(iii) The ordinates are added together in groups of 4. Having been collected at intervals of $\frac{1}{64}$ degree they now represent data collected at $\frac{1}{16}$ degree intervals. Coarser scanning steps than $\frac{1}{64}$ degree would be acceptable, but it is desirable that step (ii) should be done before (iii), *i.e.* on the finest scan step available, as misplacing the median affects the width of the peak after folding and peak width is known to be critical in relation to systematic error.

Steps (ii) and (iii) are both done by addition rather than averaging so that the $\sqrt{n}$ law remains applicable.

(iv) Results are calculated from equations (13), (15) and (16) using a profile g_2 already in the computer from previous operations, or, for the first reflexion, read in. Method *A*.

(v) Results are also calculated by the peak-minus-background method (case *B*) in which the number of ordinates in the peak region, m, is set so that all ordinates within 4σ of the median are included, where σ is the current value of the r.m.s. width of the function g_2. Method *B*.

(vi) The function g_2 is updated as follows. The background level which is now available is subtracted from the observations and any ordinate which is then negative or outside the range 4σ from the median is replaced by zero and the result normalized to sum to unity. This is taken to represent the function h_2. We then calculate a quantity γ defined by

$$\gamma = \frac{(I/I_0)^2}{1+(I/I_0)^2}, \tag{17}$$

where I_0 is a chosen constant, and replace g_2 by g_2' as follows

$$g_2' = \gamma h_2 + (1-\gamma) g_2$$

so that strong reflexions are incorporated into the learnt profile and weak ones much less so. There is no special significance in this choice of the function (17) for γ, but this function is a suitable one, easily calculated and better behaved than some alternatives, *e.g.*

$$\frac{I/I_0}{1+I/I_0}.$$

(vii) A choice is now made between the results of the two methods [steps (iv) and (v)] and if there are indications of fault conditions these can be flagged at this stage.

If, in the profile fitting method, y_{obs} and y_{calc} differ only by random noise, then the expected value of $\sqrt{R/N}$* from (13) is unity, and if it is much in excess of unity it is an indication that systematic error is present, either because g_2 has not followed changes in h_2 sufficiently closely, or because the observations are themselves perturbed, *e.g.* by electronic noise producing a spike not attributable to X-ray quanta, or to a Laue streak in the background region. In the former case (g_2 not following h_2) method *B* should be chosen, but in the other case (perturbed data) method *A* is usually better. It is not easy to distinguish these two cases on-line, but in the latter case it is usually the fact that the two methods give different answers. Accordingly, if $\sqrt{R/N}$ is large, method *B* is chosen, but a diagnostic message is also given if the methods differ.

The choice algorithm currently in use is best defined by the following flow diagram in which quantities in square brackets are computed and tested. All arrows to the right are to the output routine

* Here N relates to the reduced list of ordinates

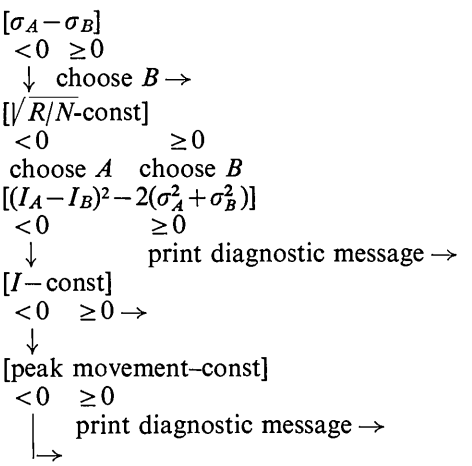

The first diagnostic message draws attention to differing results while the second traps the case in which the median-seeking routine has, in the virtual absence of a genuine peak, found a median more than 15 ordinates (out of 128) removed from the expected position (on the basis of the position of the previously processed peak on the same channel). In addition to these diagnostics there are others which detect cases in which the frame width is too narrow, or in which the peak has run up against the end of the frame, and data transmission errors (from diffractometer to computer) are also trapped by means of a check-sum.

The choice algorithm given above has been designed to be as safe as possible. In fact, it is more likely that a good measurement will have a diagnostic message attached to it than that a bad measurement will pass undetected. This is because valid measurements of very strong reflexions may be made with method B for which close agreement between the methods is not to be expected. Nevertheless, disagreements are still flagged. The program also contains a facility (hand switch controlled) for printing all 128 ordinates, and the observed, calculated and learnt profiles (16 ordinates each), which permits investigation of bad cases.

The constant with which $\sqrt{R/N}$ is compared to test ill-fitting cases is usually 1·25 or 1·125. This has been chosen by noting that values of $\sqrt{R/N}$ as low as 0·7 are not uncommon and that values below 0·6 have been observed a number of times. This shows that fluctuations (*i.e.* random noise) on the observations may fortuitously match those on g_2 to the extent of 0·3 or 0·4 in $\sqrt{R/N}$, so that, presumably, values as large as 1·3 or 1·4 could occur and still be essentially random in origin. Setting the limit at 1·25 or 1·125 is therefore conservative.

3·2. *Examples*

Table 2 shows an example of some typical results obtained by this procedure. In this Table the first column contains indices as derived from the setting of the slides on the diffractometer. The second column contains a channel number identifying the three counters used. The third and fourth columns contain I and $\sigma(I)$ for the preferred method, whichever it is. The fifth and sixth contain I and $\sigma(I)$ for the other method. The seventh contains a choice indicator and is 1 if method A (profile fitting) has been preferred and has produced the results in columns 3 and 4, and is 2 if method B has been chosen. The eighth column contains the residual $\sqrt{R/N}$, whose expected value is unity if the observed and fitted profiles differ only by random noise. The ninth column is the width from edge to centre, 4σ, of the learnt profile, expressed as a number of ordinates truncated to a multiple of four. The tenth column is the position of the peak median, in which the tendency for channel 0 to have a smaller entry here is due to the curvature of the Ewald sphere. The final column contains γ, calculated in this instance with $I_0=6144$, which is on the high side for this size of crystal.

For these measurements the background integral was about 2600 counts for channels 0 and 2 and about half that for channel 1. For channels 0 and 2 this means that profile fitting can be expected to produce a smaller variance than method B if the integrated peak counts are fewer than about 6000.

The first reflexion to be processed uses a profile supplied to the program and not learnt from this crystal. As a result, the residual, 7·185, is very high and method B is chosen in consequence. The second reflexion is then processed using the learnt image of the first for profile fitting and immediately the residual falls below 1·2 and both methods give results in close agreement. The third reflexion has a larger residual, as is usual for very strong reflexions and method B is appropriate in such cases. The fourth reflexion would, with the current version of the program, be rejected as needing remeasuring because $(I_A-I_B)^2$ exceeds $2[\sigma^2(I_A)+\sigma^2(I_B)]$. The most likely explanation for this is the presence of a white radiation streak in the background region of this reflexion, as this is an inner reflexion one removed from a reciprocal lattice axis. The large residuals for this and the remaining two channels of this setting are consistent with this explanation. The seventh and subsequent reflexions are typical and satisfactory in view of the large background, except that channel 1 for the 15−00+03+ setting should also be rejected on the grounds of disagreement between the methods.

The total number of ordinates collected for each reflexion was 128, which is a little larger than optimum for an edge to edge peak width of 56 ordinates, but is necessary to accommodate the fluctuations in median position.

Table 3 is a second example, differing from the first in that here the background integral is below 1000 counts on all three channels and the peak is a little narrower. Both of these facts reduce the advantage of method A over method B and differences between the standard deviations are accordingly smaller than previously. The constant I_0 has also been reduced to 2700,

so that the learning procedure is more responsive to change, as shown by the larger γ values. In choosing I_0 one must strike a balance between fast response (small I_0, short memory length) and the smoother learnt profile that results from compounding many observed profiles into the learnt profile (large I_0, long memory). The maximum tolerated $\sqrt{R/N}$ has also been reduced to 1·125. No disagreements have occurred.

In Fig. 2 we show one particular example of an observed and calculated profile. This is a case in which methods *A* and *B* gave substantially different results, and the reasons for the difference are worth considering. The Figure shows the 16 observed ordinates after the 128 have been folded at the median and grouped together in fours, and the division between the peak and background regions for method *B* is placed between the ninth and tenth ordinates, as indicated by the bar. The continuous curve is the fitted curve and the broken line is the learnt profile used in the fitting.

The profile fitting method gave the result 544 ± 59 and method *B* gave 816 ± 108. The difference between these is attributable to the way in which the background level is determined, and to the actual nature of the fluctuations in the ordinates. In method *B* the background level is the mean of the last 7 ordinates, which is 527, which is lower than the 544 arrived at by method *A*. The reason is that method *A* recognizes that all ordinates after the fourth are measuring *mainly* background and the fifth to ninth ordinates all exceed 527. In particular, it recognizes the ninth ordinate as subject to a positive fluctuation of about 50 counts, whereas method *B* takes it literally. If the difference between the ninth and tenth ordinates is just a random fluctuation, as it appears to be, then it is equally likely that they might have occurred the other way round, in which case method *B* would have given the result 611 instead of 816, whereas method *A* would not alter. This example illustrates the sense in which it may

Table 2. *Typical results obtained by the procedure described in* §3·1

Indices	Channel	1st choice I	1st choice $\sigma(I)$	2nd choice I	2nd choice $\sigma(I)$	Choice	$\sqrt{R/N}$	Width 4σ	Peak position	γ
*15-00+00+	2	+9388	+101	+8694	+108	+2	+7·185	+28	+80	·999
*15-00+00+	1	+5595	+77	+5614	+78	+1	+1·192	+28	+74	·453
*15-00+00+	0	+15535	+128	+15558	+128	+2	+1·784	+28	+48	·864
*15-00+01+	2	+985	+46	+796	+37	+2	+2·287	+28	+43	·016
*15-00+01+	1	+533	+33	+502	+29	+2	+1·542	+28	+44	·006
*15-00+01+	0	+1000	+46	+901	+40	+2	+1·952	+28	+35	·021
*15-00+02+	2	+999	+43	+1015	+57	+1	+0·955	+28	+50	·025
*15-00+02+	1	+736	+41	+732	+36	+2	+1·449	+28	+49	·014
*15-00+02+	0	+251	+32	+294	+49	+1	+0·766	+28	+39	·001
*15-00+03+	2	+1263	+46	+1363	+59	+1	+0·898	+28	+51	·040
*15-00+03+	1	+774	+37	+682	+42	+1	+1·022	+28	+48	·015
*15-00+03+	0	+76	+28	+135	+46	+1	+0·944	+28	+38	·000
*15-00+04+	2	+273	+32	+253	+49	+1	+0·766	+28	+55	·001
*15-00+04+	1	+178	+24	+182	+34	+1	+1·079	+28	+52	·000
*15-00+04+	0	+1306	+47	+1365	+60	+1	+1·182	+28	+43	·043
*15-00+05+	2	+558	+38	+596	+51	+1	+1·138	+28	+56	·008
*15-00+05+	1	+294	+27	+249	+36	+1	+1·102	+28	+54	·002
*15-00+05+	0	+34	+27	+43	+45	+1	+0·902	+28	+51	·000
*15-00+06+	2	+694	+38	+709	+52	+1	+1·023	+28	+57	·012
*15-00+06+	1	+390	+28	+366	+36	+1	+0·823	+28	+56	·004
*15-00+06+	0	+1288	+46	+1328	+58	+1	+1·034	+28	+46	·042
*15-00+07+	2	+797	+40	+787	+53	+1	+1·063	+28	+60	·016
*15-00+07+	1	+465	+30	+405	+38	+1	+0·819	+28	+57	·005
*15-00+07+	0	+378	+33	+361	+49	+1	+0·599	+28	+48	·003
*15-00+08+	2	+76	+28	+12	+44	+1	+1·089	+28	+54	·000
*15-00+08+	1	+68	+20	+53	+32	+1	+0·580	+28	+60	·000
*15-00+08+	0	+34	+28	+107	+46	+1	+1·228	+28	+53	·000
*15-00+09+	2	+242	+30	+245	+47	+1	+0·793	+28	+64	·001
*15-00+09+	1	+141	+23	+128	+33	+1	+0·712	+28	+60	·000
*15-00+09+	0	+138	+29	+155	+46	+1	+0·726	+28	+48	·000

be claimed that method *A* is less sensitive to random fluctuation than is method *B* and how it also gives weight to the region on the fringe of the peak, as well as the pure-background region, when determining the background level. Against this it might be said that the fault in this example lies with the learnt profile, and it is true that a wider learnt profile could account for much of the difference between the figures 544 and 611, but could not yield agreement between method *A* and 816. As it stands, however, the disagreement would yield a diagnostic message. In this example the residual is 1·22 and the peak/background ratio is 0·06.

Figs. 3 and 4 show a further comparison between methods *A*, *B* and BPB. Fig. 4 shows the percentage $\sigma(I)/I$ as a function of I for each of the three methods on the basis of the circumstances shown in Fig. 3. Methods *A* and *B* operate on the central portion in which there are 1600 background counts and the width

Table 3. *A second example of results obtained by the procedure of* §3·1 (*see text*, §3·2)

Indices	Channel	1st choice I	1st choice $\sigma(I)$	2nd choice I	2nd choice (σI)	Choice	$\sqrt{R/N}$	Width 4σ	Peak position	γ
*10+02+02+	2	+1104	+37	+1129	+40	+1	+1.106	+24	+80	.225
*10+02+02+	1	+10860	+107	+10903	+107	+2	+1.290	+24	+80	.965
*10+02+02+	0	+726	+30	+730	+34	+1	+0.741	+24	+65	.111
*10+02+01+	2	+287	+22	+295	+27	+1	+0.890	+24	+77	.019
*10+02+01+	1	+3	+11	+3	+19	+1	+1.011	+24	+70	.000
*10+02+01+	0	+3245	+61	+3246	+60	+2	+1.769	+24	+62	.715
*10+02+00−	2	+1904	+48	+1892	+46	+2	+1.140	+24	+76	.460
*10+02+00−	1	+1770	+46	+1787	+44	+2	+1.339	+24	+73	.432
*10+02+00−	0	+674	+29	+682	+33	+1	+1.040	+24	+61	.097
*10+02+01−	2	+79	+15	+101	+23	+1	+0.956	+24	+77	.001
*10+02+01−	1	+209	+19	+209	+24	+1	+0.704	+24	+73	.010
*10+02+01−	0	+3059	+58	+3054	+59	+1	+0.955	+24	+61	.690
*10+02+02−	2	+793	+32	+794	+35	+1	+0.867	+24	+74	.130
*10+02+02−	1	+1589	+42	+1587	+44	+1	+0.750	+24	+73	.375
*10+02+02−	0	+120	+16	+118	+22	+1	+1.001	+24	+59	.003
*10+02+03−	2	+298	+22	+311	+27	+1	+0.997	+24	+70	.020
*10+02+03−	1	+176	+17	+162	+22	+1	+0.880	+24	+71	.007
*10+02+03−	0	+110	+17	+132	+23	+1	+0.813	+24	+55	.002
*10+02+04−	2	+569	+28	+592	+32	+1	+0.778	+24	+72	.071
*10+02+04−	1	+2783	+55	+2782	+56	+1	+0.949	+24	+72	.648
*10+02+04−	0	+13	+13	PEAK MOVED ABRUPTLY						
*10+02+05−	2	+458	+31	+452	+26	+2	+1.151	+24	+71	.046
*10+02+05−	1	+725	+30	+712	+33	+1	+0.752	+24	+71	.111
*10+02+05−	0	+1917	+48	+1950	+47	+2	+1.498	+24	+57	.475
*10+02+06−	2	+2500	+55	+2505	+53	+2	+1.369	+24	+69	.599
*10+02+06−	1	+307	+22	+305	+27	+1	+0.961	+24	+69	.022
*10+02+06−	0	+567	+28	+545	+32	+1	+1.015	+24	+56	.071
*10+02+07−	2	+5116	+74	+5077	+76	+1	+0.776	+24	+66	.861
*10+02+07−	1	+405	+24	+426	+29	+1	+1.030	+24	+68	.037
*10+02+07−	0	+1487	+45	+1509	+42	+2	+1.243	+20	+53	.351

of the peak is half the frame width, thus allowing a positional tolerance for the peak equal to its own width. For the BPB method to operate with the same positional tolerance additional measurements corresponding to the shaded areas are made so that the BPB method is subject to a further disadvantage not represented in Fig. 4 of a factor of 2 on the data collection time or of $\sqrt{2}$ on the percentage $\sigma(I)/I$. The broken line is the limiting case common to all three methods when the background is zero.

One of the main advantages of this on-line procedure is that the number of reflexions which are measurable by any chosen criterion of precision is much increased in relation to the BPB method, and this is of great importance in the protein field in which weak reflexions are especially numerous. This is illustrated in fig. 5 for a random group of reflexions between 2·8 A and 4·5 A showing, in histogram form, the distribution of the number of reflexions measured with each accuracy. The figures 73%, 62% and 55% are the proportions of the data measured with accuracy better than 50% for each of the methods, *A*, *B* and BPB.

The other major advantage which the procedure offers is a large degree of internal consistency checking which provides traps for many conditions that might otherwise be detectable only photographically or by direct inspection of the ordinates collected.

I should like to record my indebtedness to Mr G. G. Grindley and Miss L. C. G. Goaman for their patient assistance during the proving period, to Mr R. P. Phizackerley for an input routine on which the present input routine from the counters is modelled, and to Dr U. W. Arndt for Figs. 4 and 5.

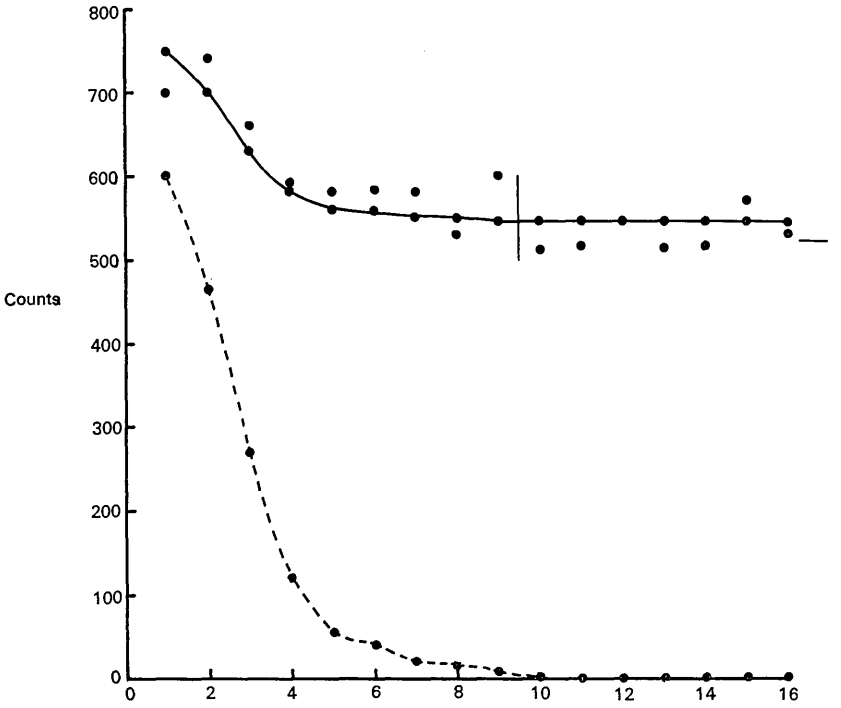

Fig. 2. An example of an observed and calculated profile. A particularly bad case (see text). The vertical bar marks the separation of peak region from background region for method *B*, and the horizontal bar is the background level as set by method *B*.

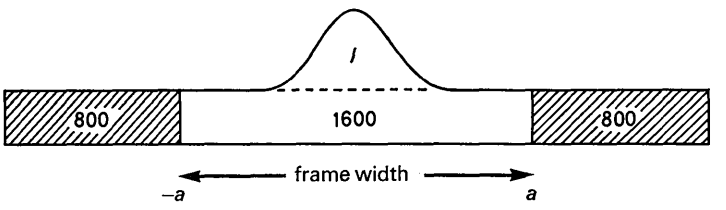

Fig. 3. Showing the basis of the comparisons made in Fig. 4. The peak is supposed to occupy half the frame width.

APPENDIX A

A study of the unweighted multi-profile case

We suppose the N observations y to be expressed by

$$\mathbf{y}=\mathbf{G}\lambda+\boldsymbol{\varepsilon}\,, \qquad (A\text{–}1)$$

in which $\mathbf{y}$ and $\boldsymbol{\varepsilon}$ are column matrices of dimension N, λ is a column of dimension $M\leq N$ and $\mathbf{G}$ is a rectangular matrix containing columns $\mathbf{g}_1,\mathbf{g}_2,\cdots\mathbf{g}_M$ which are functions being fitted to the observations. If each $\mathbf{g}$ is normalized by

$$\tilde{\mathbf{u}}\mathbf{g}_i=1 \qquad (A\text{–}2)$$

with $\tilde{\mathbf{u}}=(1,1,\cdots 1)$ and if all the elements of $\mathbf{g}_1$ are $1/N$ (representing a background function), then if λ is found by minimizing $\tilde{\boldsymbol{\varepsilon}}\boldsymbol{\varepsilon}$, λ_1 is the background integral and $\tilde{\mathbf{v}}\lambda$ is the integrated intensity where

$$\tilde{\mathbf{v}}=(0,1,1,\cdots 1),\ \text{dimension } M\,. \qquad (A\text{–}3)$$

Now the least-squares solution is

$$\lambda=(\tilde{\mathbf{G}}\mathbf{G})^{-1}\tilde{\mathbf{G}}\mathbf{y} \qquad (A\text{–}4)$$

and the integrated intensity is

$$I=\tilde{\mathbf{v}}(\tilde{\mathbf{G}}\mathbf{G})^{-1}\tilde{\mathbf{G}}\mathbf{y}\,. \qquad (A\text{–}5)$$

Now $\partial I/\partial y_i$ is the ith element of the row vector $\tilde{\mathbf{v}}(\tilde{\mathbf{G}}\mathbf{G})^{-1}\tilde{\mathbf{G}}$ and we wish to find the variance

$$\sigma^2(I)=\sum_1^N\left(\frac{\partial I}{\partial y_i}\right)^2 y_i=\tilde{\mathbf{v}}(\tilde{\mathbf{G}}\mathbf{G})^{-1}\tilde{\mathbf{G}}\mathbf{Y}\mathbf{G}(\tilde{\mathbf{G}}\mathbf{G})^{-1}\mathbf{v} \qquad (A\text{–}6)$$

where $\mathbf{Y}=\operatorname{diag}\mathbf{y}$.

It has been shown in the text (equation (10) *et seq.*) that the advantage in profile fitting arises from the fact that $\alpha\geq 1$ *i.e.* that the contribution of the background to the variance may be lower in profile fitting than in method *B*, and since this is the source of the advantage, we here attend only to the contribution of the background to the variance with a view to maximising that advantage.

Evidently the coefficient, r, of λ_1 in $\sigma^2(I)$ is, from (*A*–6)

$$r=\frac{1}{N}\tilde{\mathbf{v}}(\tilde{\mathbf{G}}\mathbf{G})^{-1}\mathbf{v}\,,$$

which is $1/N$ times the sum of all elements in $(\tilde{\mathbf{G}}\mathbf{G})^{-1}$ other than those in the first row and/or first column. Now, all elements in the first row and/or first column of $\tilde{\mathbf{G}}\mathbf{G}$ are $1/N$, therefore the sum of all the elements in any column of $(\tilde{\mathbf{G}}\mathbf{G})^{-1}$, other than the first column, vanishes, so that $\tilde{\mathbf{v}}(\tilde{\mathbf{G}}\mathbf{G})^{-1}\mathbf{v}$ is minus the sum of all the elements in the first row of $(\tilde{\mathbf{G}}\mathbf{G})^{-1}$ other than the first element. Likewise the sum of all the elements in the first row of $(\tilde{\mathbf{G}}\mathbf{G})^{-1}$ is N, so that we have finally

$$\tilde{\mathbf{v}}(\tilde{\mathbf{G}}\mathbf{G})^{-1}\mathbf{v}=(\tilde{\mathbf{G}}\mathbf{G})^{-1}_{11}-N\,,$$

or, more generally,

$$r=(\tilde{\mathbf{G}}\mathbf{G})_{11}\,(\tilde{\mathbf{G}}\mathbf{G})^{-1}_{11}-1 \qquad (A\text{–}7)$$

identifying $1/N$ with $(\tilde{\mathbf{G}}\mathbf{G})_{11}$.

$$r=\frac{\tilde{\mathbf{g}}_1\mathbf{g}_1\,||\tilde{\mathbf{g}}_i\mathbf{g}_j||}{||\tilde{\mathbf{g}}_i\mathbf{g}_j||}-1\,,$$

in which $2\leq i,j\leq M$ in the numerator and $1\leq i,j\leq M$ in the denominator. Subtracting the first row from all rows in the denominator gives

$$r=\frac{||\tilde{\mathbf{g}}_i\mathbf{g}_j||}{||\tilde{\mathbf{g}}_i\mathbf{g}_j-\tilde{\mathbf{g}}_1\mathbf{g}_1||}-1 \qquad 2\leq i,j\leq M\,.$$

Subtracting the first column from every column, leaving the first column unchanged, in each determinant gives

$$r=\frac{||\tilde{\mathbf{g}}_i\mathbf{g}_2,\ \tilde{\mathbf{g}}_i(\mathbf{g}_j-\mathbf{g}_2)||}{||\tilde{\mathbf{g}}_i\mathbf{g}_2-\tilde{\mathbf{g}}_1\mathbf{g}_1,\ \tilde{\mathbf{g}}_i(\mathbf{g}_j-\mathbf{g}_2)||}-1 \qquad \begin{matrix}2\leq i\leq M\\ 3\leq j\leq M\end{matrix}$$

$$=\frac{||\tilde{\mathbf{g}}_1\mathbf{g}_1,\ \tilde{\mathbf{g}}_i(\mathbf{g}_j-\mathbf{g}_2)||}{||\tilde{\mathbf{g}}_i\mathbf{g}_2-\tilde{\mathbf{g}}_1\mathbf{g}_1,\ \tilde{\mathbf{g}}_i(\mathbf{g}_j-\mathbf{g}_2)||}$$

$$\therefore\ \frac{r}{r+1}=\frac{||\tilde{\mathbf{g}}_1\mathbf{g}_1,\ \tilde{\mathbf{g}}_i(\mathbf{g}_j-\mathbf{g}_2)||}{||\tilde{\mathbf{g}}_i\mathbf{g}_2,\ \tilde{\mathbf{g}}_i(\mathbf{g}_j-\mathbf{g}_2)||}\,.$$

Subtracting the first row from every row and leaving the first row unchanged gives

$$\frac{r}{r+1}=\frac{\tilde{\mathbf{g}}_1\mathbf{g}_1\,||(\tilde{\mathbf{g}}_i-\tilde{\mathbf{g}}_2)\,(\mathbf{g}_j-\mathbf{g}_2)||}{\left\|\begin{matrix}\tilde{\mathbf{g}}_2\mathbf{g}_2 & , & \tilde{\mathbf{g}}_2(\mathbf{g}_j-\mathbf{g}_2)\\ (\tilde{\mathbf{g}}_i-\tilde{\mathbf{g}}_2)\mathbf{g}_2, & & (\tilde{\mathbf{g}}_i-\tilde{\mathbf{g}}_2)\,(\mathbf{g}_j-\mathbf{g}_2)\end{matrix}\right\|}\,, \quad 3\leq i,\,j\leq M\,.$$

Now resolve $\mathbf{g}_2$ into

$$\mathbf{g}_2=\mathbf{f}+\mathbf{F}$$

such that $\mathbf{F}$ is a linear combination of the functions $(\mathbf{g}_j-\mathbf{g}_2)$ $(3\leq j\leq M)$ and $\mathbf{f}$ is orthogonal to these, *i.e.*

$$\tilde{\mathbf{f}}(\mathbf{g}_j-\mathbf{g}_2)=0\,, \qquad 3\leq j\leq M\,.$$

The determinant in the denominator then becomes

$$\left\|\begin{matrix}\tilde{\mathbf{f}}\mathbf{f}+\tilde{\mathbf{F}}\mathbf{F} & , & \tilde{\mathbf{F}}(\mathbf{g}_j-\mathbf{g}_2)\\ (\tilde{\mathbf{g}}_i-\tilde{\mathbf{g}}_2)\mathbf{F}, & & (\tilde{\mathbf{g}}_i-\tilde{\mathbf{g}}_2)\,(\mathbf{g}_j-\mathbf{g}_2)\end{matrix}\right\|$$

$$=\tilde{\mathbf{f}}\mathbf{f}\,||(\tilde{\mathbf{g}}_i-\tilde{\mathbf{g}}_2)\,(\mathbf{g}_j-\mathbf{g}_2)||+\left\|\begin{matrix}\tilde{\mathbf{F}}\mathbf{F} & , & \tilde{\mathbf{F}}(\mathbf{g}_j-\mathbf{g}_2)\\ (\tilde{\mathbf{g}}_i-\tilde{\mathbf{g}}_2)\mathbf{F}, & & (\tilde{\mathbf{g}}_i-\tilde{\mathbf{g}}_2)\,(\mathbf{g}_j-\mathbf{g}_2)\end{matrix}\right\|$$

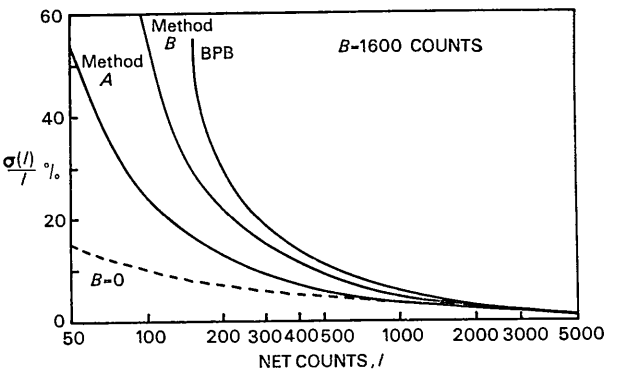

Fig. 4. Showing $\sigma(I)/I$ as a percentage as a function of I on the basis of Fig. 3, for methods *A*, *B* and *BPB*.

and the second determinant vanishes because **F** is a linear combination of the $(\mathbf{g}_j-\mathbf{g}_2)$.

$$\therefore \frac{r}{r+1}=\frac{\tilde{\mathbf{g}}_1\mathbf{g}_1}{\tilde{\mathbf{f}}\mathbf{f}} \geq \frac{\tilde{\mathbf{g}}_1\mathbf{g}_1}{\tilde{\mathbf{g}}_2\mathbf{g}_2}$$

$$r \geq \left(\frac{\tilde{\mathbf{g}}_2\mathbf{g}_2}{\tilde{\mathbf{g}}_1\mathbf{g}_1}-1\right)^{-1} \quad (A\text{–}8)$$

and the limiting case of equality occurs when $\tilde{\mathbf{g}}_2\mathbf{g}_2=\tilde{\mathbf{f}}\mathbf{f}$, *i.e.* when $\mathbf{F}=\mathbf{O}$ and $\tilde{\mathbf{g}}_2(\mathbf{g}_j-\mathbf{g}_2)=0$, $3\leq j\leq M$.

From this we conclude that increasing M, the number of curves fitted to the observations, beyond 2 must increase r, thereby eroding the advantage of curve fitting, unless $\mathbf{g}_3\cdots\mathbf{g}_M$ all satisfy

$$\tilde{\mathbf{g}}_2(\mathbf{g}_j-\mathbf{g}_2)=0\,. \quad (A\text{–}9)$$

We now proceed to consider a system with $M\geq 3$ within the condition (*A*–9) and with a view to permitting the fitted curve $\mathbf{G}\lambda$ to fit observed curves of a variety of shapes.

The normal matrix $\tilde{\mathbf{G}}\mathbf{G}$ is then of the form

$$\begin{pmatrix} \tilde{\mathbf{g}}_1\mathbf{g}_1 & \tilde{\mathbf{g}}_1\mathbf{g}_1 & \tilde{\mathbf{g}}_1\mathbf{g}_1 & \tilde{\mathbf{g}}_1\mathbf{g}_1 \\ \tilde{\mathbf{g}}_1\mathbf{g}_1 & \tilde{\mathbf{g}}_2\mathbf{g}_2 & \tilde{\mathbf{g}}_2\mathbf{g}_2 & \tilde{\mathbf{g}}_2\mathbf{g}_2 \\ \tilde{\mathbf{g}}_1\mathbf{g}_1 & \tilde{\mathbf{g}}_2\mathbf{g}_2 & \tilde{\mathbf{g}}_3\mathbf{g}_3 & \tilde{\mathbf{g}}_3\mathbf{g}_4 \\ \tilde{\mathbf{g}}_1\mathbf{g}_1 & \tilde{\mathbf{g}}_2\mathbf{g}_2 & \tilde{\mathbf{g}}_4\mathbf{g}_3 & \tilde{\mathbf{g}}_4\mathbf{g}_4 \end{pmatrix}$$

for $M=4$. The first two rows and columns are now special and the remaining ones are not. For brevity we write

$$(\tilde{\mathbf{G}}\mathbf{G})=\begin{pmatrix} a & a & a & a \\ a & b & b & b \\ a & b & c & d \\ a & b & d & e \end{pmatrix} \quad (\tilde{\mathbf{G}}\mathbf{G})^{-1}=\begin{pmatrix} q & r & s & t \\ r & u & v & w \\ s & v & x & y \\ t & w & y & z \end{pmatrix}$$

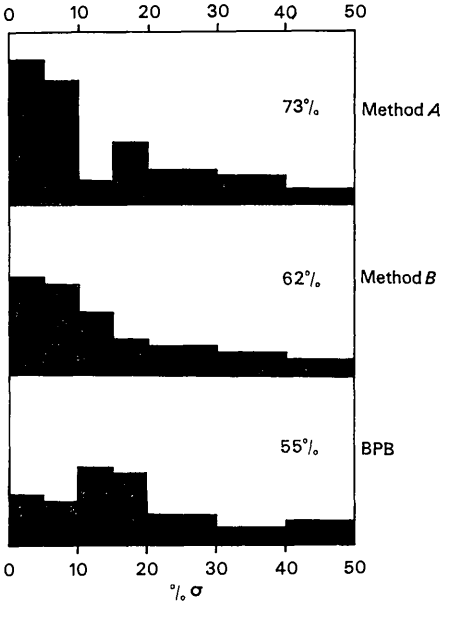

Fig. 5. Histograms showing the distribution of the number of reflexions occurring with a given precision for each of the three methods.

Multiplying the 1st row of $\tilde{\mathbf{G}}\mathbf{G}$ by the 1st column of $(\tilde{\mathbf{G}}\mathbf{G})^{-1}$ gives

$$a(q+r+s+t)=1\,.$$

Multiplying the 2nd row of $\tilde{\mathbf{G}}\mathbf{G}$ by the 1st column of $(\tilde{\mathbf{G}}\mathbf{G})^{-1}$ gives

$$aq+b(r+s+t)=0 \quad \therefore r+s+t=\frac{1}{a-b}\,.$$

Multiplying the 1st row of $\tilde{\mathbf{G}}\mathbf{G}$ by the 2nd column of $(\tilde{\mathbf{G}}\mathbf{G})^{-1}$ gives

$$a(r+u+v+w)=0\,.$$

Multipying the 2nd row of $\tilde{\mathbf{G}}\mathbf{G}$ by the 2nd column of $(\tilde{\mathbf{G}}\mathbf{G})^{-1}$ gives

$$ar+b(u+v+w)=1 \quad \therefore u+v+w=\frac{1}{b-a}\,.$$

Multiplying the 1st row of $\tilde{\mathbf{G}}\mathbf{G}$ by the 3rd column of $(\tilde{\mathbf{G}}\mathbf{G})^{-1}$ gives

$$a(s+v+x+y)=0\,.$$

Multiplying the 2nd row of $\tilde{\mathbf{G}}\mathbf{G}$ by the 3rd column of $(\tilde{\mathbf{G}}\mathbf{G})^{-1}$ gives

$$as+b(v+x+y)=0 \quad \therefore v+x+y=0 \quad \text{unless } a=b.$$

(*A*–5) now gives us

$$I=\tilde{\mathbf{v}}(\tilde{\mathbf{G}}\mathbf{G})^{-1}\tilde{\mathbf{G}}\mathbf{y}=\left(\frac{1}{a-b}\,,\ \frac{1}{b-a}\,,\ 0,0\right)\tilde{\mathbf{G}}\mathbf{y}$$

$$=\frac{1}{a-b}(\tilde{\mathbf{g}}_1-\tilde{\mathbf{g}}_2)\mathbf{y}=\frac{\tilde{\mathbf{g}}_1-\tilde{\mathbf{g}}_2}{\tilde{\mathbf{g}}_1\mathbf{g}_1-\tilde{\mathbf{g}}_2\mathbf{g}_2}\,\mathbf{y}$$

and the generalization for all $M\geq 3$ is obviously the same.

This expression is identical with the expression obtained when $M=2$ (*cf.* Appendix B), *i.e.* when we fit a background and a single curve to the observations. Therefore we have proved that if we fit a background and more than one curve to the observations (with a view to avoiding systematic errors) then either

(i) The expression for I is unchanged so that its susceptibility to systematic error is also unchanged or

(ii) r increases so that the contribution of the background to the variance is more than minimal.

It follows that the shape of g_2 alone is relevant and all important, and that the only possibility of minimizing the variance *and* of avoiding systematic error is to use the *single* curve g_2 and arrange for its shape to match the shape of the observed profile in the sense that $\tilde{\mathbf{g}}_2\mathbf{g}_2=\tilde{\mathbf{g}}_2\mathbf{h}_2$, as shown in Appendix B.

APPENDIX B

In this Appendix we obtain formulae for I and $\sigma^2(I)$ when fitting a constant function g_1 and a single profile curve g_2 to the unweighted observations for the general case and for the two special cases discussed in the text.

Equation (*A*–5) for the case $M=2$ reduces immediately to

$$I=\frac{\tilde{\mathbf{g}}_1-\tilde{\mathbf{g}}_2}{\tilde{\mathbf{g}}_1\mathbf{g}_1-\tilde{\mathbf{g}}_2\mathbf{g}_2}\,\mathbf{y} \qquad (B\text{–}1)$$

because

$$\tilde{\mathbf{g}}_1\mathbf{g}_2=\tilde{\mathbf{g}}_1\mathbf{g}_1=1/N\,.$$

Now suppose

$$\mathbf{y}=\mathbf{h}_1\mu_1+\mathbf{h}_2\mu_2\,, \qquad (B\text{–}2)$$

in which $\mathbf{h}_1$ again represents the background function and $\mathbf{h}_2$ the shape, both being normalized according to (*A*–2), so that necessarily

$$\mathbf{h}_1=\mathbf{g}_1\,;$$

then combining (*B*–1) and (*B*–2) gives

$$I=\mu_2\frac{\tilde{\mathbf{g}}_1\mathbf{g}_1-\tilde{\mathbf{g}}_2\mathbf{h}_2}{\tilde{\mathbf{g}}_1\mathbf{g}_1-\tilde{\mathbf{g}}_2\mathbf{g}_2}=\mu_2\frac{N\tilde{\mathbf{g}}_2\mathbf{h}_2-1}{N\tilde{\mathbf{g}}_2\mathbf{g}_2-1} \qquad (B\text{–}3)$$

so that I is a true measure of the integrated intensity μ_2 if and only if $\tilde{\mathbf{g}}_2\mathbf{h}_2=\tilde{\mathbf{g}}_2\mathbf{g}_2$.

For the variance $\sigma^2(I)$ we take equations (*A*–6) and (*B*–1) giving

$$\sigma^2(I)=\frac{\tilde{\mathbf{g}}_1-\tilde{\mathbf{g}}_2}{(\tilde{\mathbf{g}}_1\mathbf{g}_1-\tilde{\mathbf{g}}_2\mathbf{g}_2)}\,\mathbf{Y}\,\frac{\mathbf{g}_1-\mathbf{g}_2}{(\tilde{\mathbf{g}}_1\mathbf{g}_1-\tilde{\mathbf{g}}_2\mathbf{g}_2)}$$

or, using a notation in which $\tilde{\mathbf{g}}_1^2$ is a row vector, the ith element of which is the square of the ith element of $\tilde{\mathbf{g}}_1$, we have

$$\sigma^2(I)=\frac{\tilde{\mathbf{g}}_1^2-2\widetilde{\mathbf{g}_1\mathbf{g}_2}+\tilde{\mathbf{g}}_2^2}{(\tilde{\mathbf{g}}_1\mathbf{g}_1-\tilde{\mathbf{g}}_2\mathbf{g}_2)^2}\,\mathbf{y}\,,$$

which, on inserting (*B*–2) and recalling that each element of $\mathbf{g}_1$ and $\mathbf{h}_1$ is $1/N$, gives

$$\sigma^2(I)=\mu_1\frac{1}{N\tilde{\mathbf{g}}_2\mathbf{g}_2-1}+\mu_2\frac{1-2N\tilde{\mathbf{g}}_2\mathbf{h}_2+N^2\tilde{\mathbf{g}}_2^2\mathbf{h}_2}{[N\tilde{\mathbf{g}}_2\mathbf{g}_2-1]^2}\,. \qquad (B\text{–}4)$$

Equations (*B*–3) and (*B*–4) are for the general case *A* in Table 1. For case *B* we suppose that g_2 is constant within the peak region and equal to $1/m$ where m is the number of peak ordinates, and is zero in the background region of $n=N-m$ ordinates. Then, assuming only that h_2 vanishes in the background region but is normalized and of any shape, substitution in (*B*–3) and (*B*–4) gives immediately

$$I=\mu_2 \quad \text{and} \quad \sigma^2(I)=\mu_1\frac{m}{n}+\mu_2\,. \qquad (B\text{–}5)$$

For case *C* of Table 1, g_2 and h_2 represent Gaussians, and for analytical purposes it is convenient to replace sums such as $\tilde{\mathbf{g}}_2\mathbf{g}_2$ by corresponding integrals. Suppose that the working range containing N ordinates is of width $2a$ in the continuous variable x which forms the abscissa, so that successive ordinates are separated by an interval $\delta x=2a/N$ and let each function g or h have primed counterparts which are continuous such that

$$\int_{-a}^{a}g'dx=1\,;$$

then the continuous function is related to the discrete one by

$$g'\delta x=g\,,$$

assuming the sampling interval is fine enough to allow this. Then

$$\tilde{\mathbf{g}}_2\mathbf{g}_2=\Sigma\,g_2^2=\frac{1}{\delta x}\int_{-a}^{a}(g_2'\delta x)^2dx=\delta x\int_{-a}^{a}g_2'^2dx\,;$$

similarly

$$\tilde{\mathbf{g}}_2^2\mathbf{h}_2=(\delta x)^2\int_{-a}^{a}g_2'^2h_2'dx\,.$$

Setting

$$g_2'=\frac{1}{p}\exp(-\pi x^2/p^2)\equiv f(p,x)$$

$$h_2'=\frac{1}{q}\exp(-\pi x^2/q^2)\equiv f(q,x)\,,$$

then using the property that

$$f(p,x)f(q,x)=(p^2+q^2)^{-1/2}f[(p^{-2}+q^{-2})^{-1/2},\,x]$$

leads at once to

$$I=\mu_2\frac{2a\sqrt{\frac{2p^2}{p^2+q^2}}-p\sqrt{2}}{2a-p\sqrt{2}} \qquad (B\text{–}6)$$

and

$$\sigma^2(I)=\mu_1\frac{1}{2a/p\sqrt{2}-1}+\mu_2\cdot\frac{1-\frac{4a}{\sqrt{p^2+q^2}}+\frac{4a^2}{p\sqrt{p^2+2q^2}}}{[2a/p\sqrt{2}-1]^2} \qquad (B\text{–}7)$$

Reference

GOSSLING, T. H. (1967). *Acta Cryst.* **22**, 465.

DISCUSSION

HOPPE: Can your method deal with the α-doublet?

DIAMOND: In principle, yes, but there are some practical difficulties. The program must be able to deal with a varying position of the peak within the frame; hence the first step is to fold the profile about the median ordinate. So long as the program locks unequivocally on to the same part of the profile there is no basic difficulty. We do not go out to Bragg angles where the α-doublet is resolved: the nearest analogous situation was one in which the crystal was split. Here the program clearly detected the splitting of the profile.

JOHNSON: How do you deal with very rapidly changing profiles, such as when the crystal planes are curved?

DIAMOND: In the early days we used a scan along reciprocal lattice lines where we had a rapid variation of spot shape

owing to rapid changes in the Lorentz factor. At that time we tried to use the trend, that is the rate of change, of the profile. We now use an ω scan where this is not worth while since we measure the reflexions in an orderly sequence along a zigzag path through the lattice. The reciprocal lattice lines are very crowded, and so the change in profile from one reflexion to the next is slow. With more widely separated reflexions it might be necessary to take the trend into account.

COPPENS: How do you start the process?

DIAMOND: The program is primed with a hypothetical profile. The first one or two reflexions are thus badly matched until the program has learnt a better approximation.

HAMILTON: Is it necessary to be connected on-line to a computer? You are not using the computer to make running alterations.

DIAMOND: You could record the 128 ordinates of each reflexion on an off-line magnetic tape; the computer is most useful in reducing the output.

Acta Cryst. (1969). A**25**, 55 B2·1

Present Problems and Future Opportunities in Precise Intensity Measurements with Single-Crystal X-ray Diffractometers*

BY R. A. YOUNG

Georgia Institute of Technology, Atlanta, Georgia 30332 *U.S.A.*

Considerable progress is foreseen toward the precise determination of integrated X-ray reflection intensities from small single crystals. High on the list of presently-limiting problems are multiple reflection, extinction, thermal diffuse scattering, unnecessary other background, counting statistics, effective integration and specimen change. Specific recommendations for equipment design and use are made which will partially alleviate each of them. Opportunities for better utilization of existing equipment through improved strategies for data collection and employment of small on-line computers are pointed out.

Introduction

Accurate determination of Bragg intensities and structure factors depends both on well-designed diffractometric experiments and on application of corrections for factors not subject to experimental control. In the context of integrated intensities and small single crystals, this paper is concerned with the good design of the experiments, of which there are two principal and interacting aspects, equipment design and measurement strategy. Recent years have brought considerable progress, particularly in equipment design, and precision in the 2 or 3% range has become almost routine (Abrahams, Alexander, Furnas, Hamilton, Ladell, Okaya, Young & Zalkin, 1967; Ladell, 1965; Young & Sudarsanan, 1968; Zachariasen & Plettinger, 1965). However, there are several only partially solved problems and a number of opportunities for which significant progress can yet be expected in the foreseeable future. The problems discussed here are multiple reflection, extinction, thermal diffuse scattering, other background content, counting statistics, effective integration, and specimen change, *e.g.* annealing, radiation damage or deterioration. For each problem, one or more directions for experimental progress are indicated and, where appropriate, forward reference is made to other papers in this conference. Areas of opportunity discussed include (1) improvements in diffractometer design to provide more efficient use of the incident flux, (2) optimization of the data-collection strategy for the particular purpose (*e.g.* parameter) of interest and to assist in data validation, handling and reduction, and (3) control of specimen-environmental parameters as part of the diffraction experiment. Some comments about the purposes to be served by, and requirements of, on-line computers are included.

* Work supported in part by the U S. Public Health Service through NIH-NIDR Grant DE 01912.

Multiple reflection

Though recognized for many years (Renninger, 1937), multiple reflection has only recently begun to be seriously considered as a source of significant errors in 'routine precision' measurements of Bragg intensities. When two or more reciprocal lattice points are in contact with the Ewald sphere at the same time, intensity is reflected out of the stronger beams into the weaker ones. The degree to which this occurs depends on the number of reflections operating at once, the strengths of the coupling reflections, and on much the same parameters, especially mosaic spread, as are important to secondary extinction (Zachariasen, 1967). In a hypothetical extreme case, as Zachariasen (1965*a*,*b*) has pointed out, the result could be to make all reflections appear to have the same intensity. In practice, as Zachariasen has shown theoretically and Post (this